Memory effects of local flame dynamics in turbulent premixed flames

Thorsten Zirwes[a,b,c,*], Feichi Zhang[b], Henning Bockhorn[b]

[a] *Steinbuch Centre for Computing, Karlsruhe Institute of Technology, Hermann-von-Helmholtz-Platz 1, 76344 Eggenstein-Leopoldshafen, Germany*
[b] *Engler-Bunte-Institute, Division of Combustion Technology, Karlsruhe Institute of Technology, Engler-Bunte-Ring 1, 76131 Karlsruhe, Germany*
[c] *Department of Mechanical Engineering, Stanford University, Stanford CA 94305, USA*

Abstract

A premixed and thermo-diffusively unstable turbulent hydrogen-air flame-in-a-box case is simulated in conjunction with the flame particle tracking (FPT) method. The flame is located in the flamelet regime. The focus lies on the assessment of memory effects in local flame dynamics. By tracking flame particles on an iso-surface of the flame during flame-turbulence interaction, the time history of flame speed and flame stretch can be recorded for each point on the flame iso-surface in a Lagrangian reference frame. The results reveal a time delay between the local flame speed and flame stretch signal, showing that previous values of flame stretch affect currently observed values of flame speed. Furthermore, by choosing flame particles whose trajectories are dominated by single frequencies, the time delay can be quantified. While plotting instantaneous values of flame speed and flame stretch results in a large scattering for turbulent flames, a quasi-linear correlation can be achieved by shifting the time signal of flame stretch according to the time delay. The time delay itself depends on the local flow time scale, which is expressed as a local Damköhler number. There is, however, an important difference between consumption and displacement speed. While most analyses in the literature are limited to the flame displacement speed, the flame consumption speed is evaluated for each flame particle in this work as well, which shows a strong correlation with the local equivalence ratio even at unsteady conditions. As the flame particles move toward regions with more negative flame stretch, the consumption speed decreases as the flame locally extinguishes. At the same time, the diffusive component of the displacement speed increases, as the tangential component of the diffusive flux increases in regions with strong negative flame curvature.

Keywords: Flame Particle Tracking; Flame Dynamics; Turbulent Premixed Flames; Flame Stretch; Memory Effects

1. Introduction

The interaction of turbulent flow with flames constitutes a complex problem that spans many orders of magnitudes of relevant length and time scales and is governed by a large number of physical processes, e.g. chemical reactions, molecular diffusion, turbulent velocity fluctuations and their mutual interaction. Because of this, turbulence-flame interaction is still not fully understood.

A fundamental property of flames is the flame speed s. For laminar, steady-state flames, the flame speed can be expressed as a function of the flame stretch K or normalized flame stretch Ka, which represents a laminar Karlovitz number [2]. Figure 1 on the left shows the correlation of local flame speed s, normalized by the laminar, unstretched flame speed $s_{L,0}$, and the normalized flame stretch for a hydrogen-air Bunsen flame from [1]. This allows a simple modeling of the flame speed as a quasi-linear function of Ka. For turbulent flames, however, this simple correlation is not valid anymore [3, 4]. Figure 1 on the right shows value pairs of flame speed and flame stretch on different points on a turbulent hydrogen-air flame iso-surface discussed further below. A strong scattering of the data is observed, which is typical of transient flames. However, this effect cannot be reliably modeled with the current understanding [5–10].

One possible reason for the scattering of the flame speed s and flame stretch K correlation in transient flames is that instantaneously observed values of s are affected by prior values of K. This type of memory effect or the time history of local flame dynamics cannot be assessed by evaluating single time snapshots of the flame in an Eulerian reference frame, as shown on the right of Fig. 1. Nevertheless, this is the most common way of evaluating direct numerical simulations of turbulent combustion. Instead, a Lagrangian reference frame has to be employed, where single points on the flame surface are tracked over time to reveal the thermo-chemical trajectories of the local flame dynamics.

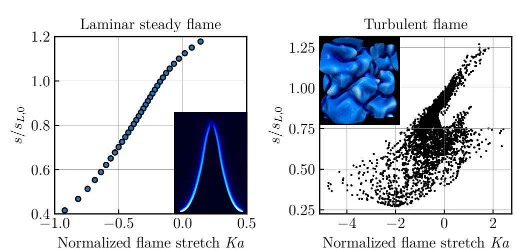

Fig. 1: Correlation of local flame speed with flame stretch of hydrogen-air flames. Left: Laminar steady-state rich Bunsen flame from [1]. Right: Lean turbulent flame from this work. The picture on the left shows the heat release rate field in the Bunsen flame and the picture on the right depicts an iso-surface of hydrogen in the turbulent flame.

The numerical tool for the investigation of flames in a co-moving Lagrangian reference frame has been devised by Chaudhuri [11]. So called flame particles (FPs) represent material points on an iso-surface of the flame. They are tracked during the simulation and record time signals of e.g. flame speed and flame stretch on well defined points on the flame surface, thus enabling to include the time history in the analysis of local flame dynamics. Flame particles have been used in the past both in turbulent flames [11–14] as well as laminar flames [1].

The aim of this work is to utilize flame particles to study the correlation of flame speed and flame stretch in a turbulent hydrogen-air flame in the flamelet regime with focus on the memory effect in the local flame dynamics. The goal is to recover a quasi-linear correlation from the strongly scattered data by taking the time histories of flame speed and flame stretch on material points on the flame front into account. In contrast to previous works that were mostly limited to evaluating the flame speed in terms of the displacement speed, this work combines the flame particle tracking technique with the evaluation of the local consumption speed, which is much more expensive computationally because a line integral has to be evaluated at every point on the flame surface. A turbulent flame setup is chosen over a laminar one for two main reasons: a) with a single turbulent simulation, flame-flow interaction over a broadband of length and time scales can be realized; b) the configuration ensures that the flame particles experience a realistic combination of curvature and strain. For typical laminar flame configurations, either only positive flame stretch occurs (e.g. in counterflow flames) or only stretch due to curvature (e.g. spherically expanding flames).

This work is organized as follows: section 2 gives a brief description of the mathematical fundamentals of flame particles. The numerical setup for the turbulent premixed hydrogen-air flame is given in section 3. Section 4 validates the flame particle trajectories with characteristics known from the literature. The assessment of the memory effect on local flame dynamics is presented in section 5. Section 6 demonstrates the difference between consumption speed and displacement speed in the context of the flame particle tracking method. The findings are summarized in section 7.

2. Fundamentals of Flame Particles

Flame particles (FPs) are massless, sizeless, virtual tracer particles that follow material points on flame iso-surfaces and do not interact with the flame or the flow. Because FPs co-move with an iso-surface of the scalar φ, their movement is described by $\frac{\mathrm{d}\varphi}{\mathrm{d}t} = 0$. From this, the movement velocity $\vec{w}$ of any material point or FP can be shown to be [1, 11, 15]

$$\vec{w} = \vec{u} + s_d \vec{n}, \tag{1}$$

where $\vec{u}$ is the fluid velocity and $\vec{n} = \nabla\varphi/|\nabla\varphi|$ the surface unit normal vector. The normalized displacement speed $s_d^* = s_d\rho/\rho_0$ evaluated for an iso-surface of the fuel mass fraction Y_F is given by

$$s_d^* = \underbrace{\frac{-\dot{\omega}_F}{\rho_0|\nabla Y_F|}}_{s^*_{d,\text{chem}}} + \underbrace{\frac{\nabla \cdot \vec{j}_F}{\rho_0|\nabla Y_F|}}_{s^*_{d,\text{diff}}}, \tag{2}$$

where $\dot{\omega}_F$ is the reaction rate of the fuel species F, ρ the gas mixture density, ρ_0 the density of the unburnt gas, $\vec{j}_F$ the diffusive flux of the fuel, $s^*_{d,\text{chem}}$ the component of s_d^* due to chemical reactions and $s^*_{d,\text{diff}}$ the component due to diffusion. The diffusive contribution can be further split into a normal and tangential component

$$s^*_{d,\text{diff}} = \underbrace{-\frac{\rho}{\rho_0} D_{m,F} \nabla \cdot \vec{n}}_{s^*_{d,\text{diff,tang}}} \underbrace{- \frac{1}{\rho_0|\nabla Y_F|}\frac{\partial}{\partial n}\left(\rho D_{m,F}\frac{\partial Y_F}{\partial n}\right)}_{s^*_{d,\text{diff,norm}}}, \tag{3}$$

where it is assumed that the diffusive flux of species F is expressed as $\vec{j}_F = -\rho D_{m,F}\nabla Y_F$ and $D_{m,F}$ is the mixture-averaged diffusion coefficient. The local consumption speed s_c is computed from a line integration normal to the flame front according to

$$s_c = \frac{\int \dot{\omega}_F \, \mathrm{d}n}{\rho_0(Y_{F,b} - Y_{F,0})}, \tag{4}$$

where $Y_{F,0}$ is the fuel mass fraction in the unburnt mixture and $Y_{F,b}$ the one in the burnt mixture.

The concept of flame stretch is related to the movement of FPs by

$$Ka = \nabla_t \cdot \vec{w}\,\tau_c = \underbrace{\nabla_t \cdot \vec{u}\,\tau_c}_{Ka_s} + \underbrace{s_d \nabla \cdot \vec{n}\,\tau_c}_{Ka_c}, \tag{5}$$

where ∇_t is the gradient tangential to the iso-surface, Ka_s the non-dimensional strain, Ka_c the non-dimensional flame stretch due to propagation of a curved surface and $\tau_c = \delta_{th,0}/s_{L,0}$ the reference flame transit time of an unstretched flame with thermal thickness $\delta_{th,0}$.

3. Computational Setup

The turbulent premixed flame considered in this work is located in the flamelet regime and operated at atmospheric conditions with an equivalence ratio of $\phi = 0.5$, which corresponds to a laminar flame with $s_{L,0} = 55.6$ cm/s, $\delta_{th} = 0.42$ mm and $\tau_c = 0.75$ ms. This flame has been selected for the relevancy of hydrogen in near-future carbon-free energy systems.

The computational domain is a rectangular box, which can be regarded as a section of a larger turbulent flame, with dimensions of $L_x \times L_y \times L_z = 2\,\text{cm} \times 1\,\text{cm} \times 1\,\text{cm}$, where x is the direction of the main flow. The domain length has been chosen after running a preliminary simulation on a domain half the length, which is available as an animation in the supplementary materials. At the inlet (see Fig. 2), a turbulent inlet generator [16] creates the inflow with prescribed turbulence parameters (bulk velocity $\bar{u}/s_{L,0} = 4.5$, fluctuation scale $u'/s_{L,0} = 3.4$, integral length scale $L_t/\delta_0 = 30$, with $\delta_0 = 0.066$ mm being the diffusive thickness). The integral turbulence turnover time is about 1 ms. These conditions are selected to retain the flame within the computational domain during its propagation. On the opposite side of the box, there is an outlet enforcing zero-gradients. The four lateral sides constitute cyclic boundary conditions. The mesh consists of $719 \times 359 \times 359$ cells, which yields an equidistant resolution of $\delta_{th,0}/\Delta x = 15$ or in terms of the Kolmogorov length $l_K/\Delta x = 2.5$ (see also Table 1). The simulation is run for a total of 24 ms, $32\tau_c$, 24 integral turbulence turnover times or 3 flow-through times based on the inlet conditions. All flame particle trajectories are recorded for 5 ms $< t <$ 20 ms, after which the flame approaches the inlet plane. The maximum extend of the flame brush between $t = 5$ ms and $t = 15$ ms is about 40 % of the domain length. Iso-surfaces illustrating the position of the flame front at different time instances are available in the supplementary materials.

The simulation is conducted with an in-house code [9, 17–21] based on OpenFOAM [22] and Cantera [23]. It employs the finite volume method to solve the fully compressible Navier–Stokes equations. Chemical reaction rates are computed with the finite rate chemistry model based on the detailed reaction mechanism by Li et al. [24] and molecular diffusion for all species is considered with the mixture-averaged diffusion model. Spatial derivatives are computed with fourth-order interpolation schemes and temporal discretization is implicit and second-order. The time step is dynamically adjusted to keep the convective CFL number below 0.1.

3.1. Flame particle seeding and selection

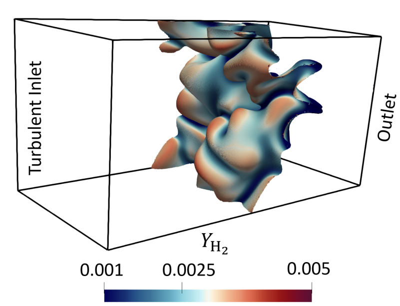

Fig. 2: Computational domain. A turbulence generator at the inlet (left) creates the turbulent flow that interacts with the flame, shown here as temperature iso-surface $T = 1050$ K colored by Y_{H_2}.

Table 1: Summary of physical parameters for the turbulent flame simulation.

Quantity	Value
Laminar thermal flame thickness δ_{th} (mm)	0.42
Laminar flame speed $s_{L,0}$ (cm/s)	55.6
Laminar diffusive flame thickness δ_0 (mm)	0.07
Flame transit time $\tau_c = \delta_{th}/s_{L,0}$ (ms)	0.75
Kolmogorov length l_K (μm)	70
Lewis number $Le = D_{\mathrm{O_2}}/D_{\mathrm{H_2}}$	0.46
Normalized velocity fluctuations $u'/s_{L,0}$	3.4
Normalized integral length scale L_t/δ_0	30
Normalized unburnt mean bulk flow velocity $\bar{u}/s_{L,0}$	4
Turbulent Damköhler number $Da_t = (L_t/u')/(\delta_0/s_{L,0})$	8
Turbulent Karlovitz number $Ka_t = \delta_0^2/l_K^2$	0.89

Flame particles are randomly seeded on an iso-surface of the fuel mass fraction $Y_{\mathrm{H_2,iso}} = 0.0032$ that corresponds to the mass fraction value at the position of the maximum heat release rate in an unstretched laminar flame. During the simulation, the FPs are tracked on the iso-surface and time signals of flame speed, flame stretch and other quantities are recorded to reveal the effect of unsteady fluctuations on local flame dynamics. The flame particles are seeded every 0.5 ms onto random points on the iso-surface. In total, about 500 000 flame particles are tracked over the course of the full simulation. Tracking is started 5 ms after the start of the simulation and particles that approach any boundary within 0.5 mm are removed.

For the analyses performed in section 4, 50 000 flame particle trajectories are chosen at random. For the discussion in section 5, the following selection criteria are applied:

- the particle lifetime τ_p is longer than $0.01\tau_c$
- the flame stretch experienced by the FP is limited to $|Ka| < 5$ throughout the particle's lifetime
- there is one value of flame stretch that is encountered twice throughout the particle's lifetime with a total change of flame stretch of $(\max(Ka) - \min(Ka)) > 0.5$ in-between, so that a meaningful trajectory in the flame speed and flame stretch space is represented.

Throughout the simulation, about 500 flame particles fulfill the above mentioned criteria. Because these flame particles experience a moderate range of flame stretch, they are expected to follow the linear Markstein correlation. Additionally, these particle trajectories are dominated by single frequencies (see section 5).

4. Characteristic Lifetime of Flame Particles

Chaudhuri [11] found that flame particles tend to follow a characteristic lifetime: During the first roughly 90 % of their lifetime, flame particles are characterized by moderate values of flame speed and flame stretch. During the last 10 % of their lifetime, they move into regions with strong negative curvature and a steep increase of the displacement speed until they are annihilated [4, 11–13, 25]. The same analysis is performed in this work, but here for a lean, thermo-diffusively unstable hydrogen-air flame. Additionally, the local consumption speed has been included in the analysis.

Figure 3 depicts time signals of different quantities recorded by a single FP tracking a point on the turbulent flame's iso-surface showing the flame particle characteristic life. The FP starts out in a region with moderate flame stretch $|Ka| < 1$ (bottom left). Because of the connection between material points and flame stretch (flame particles move with $\vec{w}$ and flame stretch is generated by $K = \nabla_t \cdot \vec{w}$, see Eqs. (1) and (5)), flame particles tend to move to regions with negative flame stretch, so that the overall non-dimensional flame stretch Ka becomes more negative over time, with the characteristic sharp drop near the end of the FP lifetime. Because a lean hydrogen flame is considered here, more negative flame stretch causes lower local equivalence ratios and thus weakens the chemical reaction rates. Because of this, s_c on the top left of Fig. 3 and the chemical contribution to s_d^* on the top right go toward zero as the flame locally extinguishes in regions with strong negative curvature. At the same time, the overall displacement speed increases, which is driven by a strong increase of the tangential component of the diffusive flux (orange line at the top right), which causes a change of the sign of $s_{d,\mathrm{diff}}^*$ from negative in moderate flame stretch regions to positive in strongly curved regions (the same holds for the diffusive flux of H_2, see the blue line on the bottom right).

5. Lagrangian Viewpoint and Memory Effects

Studying the effect of time histories on local flame dynamics is only possible by employing a Lagrangian reference frame provided by the flame particles. Figure 4 at the top shows the correlation of $s_c/s_{L,0}$ and

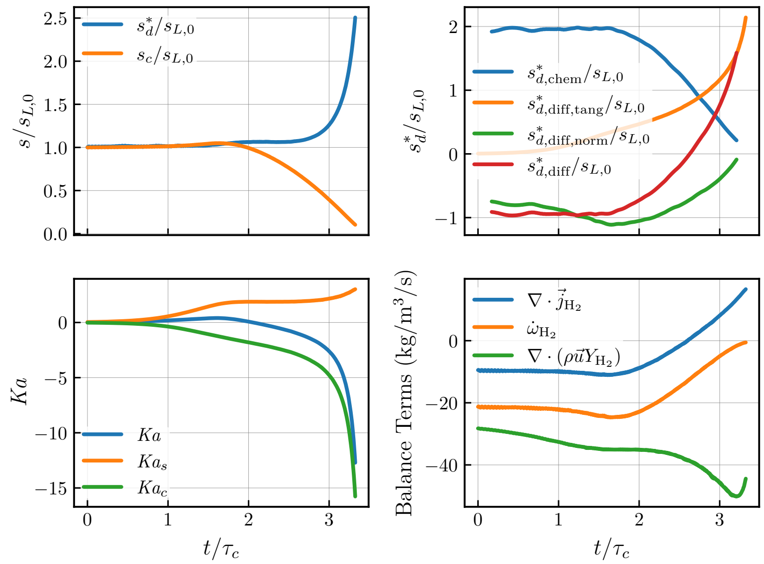

Fig. 3: Time signals of flame speed in terms of s_c and s_d^* (top left), components of displacement speed (top right), flame stretch (bottom left) and the terms of the hydrogen mass fraction balance equation (bottom right) of a single FP.

Ka in the Eulerian reference frame. This means that each point in the figure represents the instantaneous values of flame speed and flame stretch at many different points along the flame evaluated from different time snapshots where the flame is considered frozen. In this way, it is not possible to establish a causal temporal connection between the points. In contrast to that, Fig. 4 on the bottom presents the same correlation, but in the Lagrangian reference frame. Instead of picking arbitrary points at different time snapshots, each flame particle tracks a defined point on the flame iso-surface over time. Each colored line in the bottom figure represents the trajectory of a FP while following a single point on the flame surface over time, shown in flame speed and flame stretch space. In this viewpoint, the temporal evolution of flame dynamics becomes visible. The cluster of flame particles from Fig. 4 has been chosen for the following analysis because it tracks a segment of the flame whose dynamics are dominated by single frequencies for the lifetime of the flame particles. The strong scattering of flame speed and flame stretch leads to a low Pearson correlation coefficient of $\varrho = 0.68$. Note that the focus here lies on the analysis flame consumption speed s_c, as explained in the next section.

Figure 5 shows the trajectory of a single FP from the cluster of particles in Fig. 4, i.e. the line in the top part of Fig. 5 represents a single trajectory from the bottom part of Fig. 4. Instead of displaying the trajectory of the FP in flame speed and flame stretch space (top of Fig. 5), the time signal of normalized flame stretch $Ka(t)$ and normalized flame speed $s_c(t)/s_{L,0}$ of that FP is depicted on the bottom. In this way, a time lag Δt between the time signal of $Ka(t)$ (red line) and $s_c(t)$ (blue line) becomes visible, which shows that instantaneous values of s_c are affected by previous values of Ka. Because time histories of s_c and Ka are available for each material point on the flame surface due to the flame particle tracking, the time lag Δt can be evaluated for each FP from the cluster.

To determine Δt, the time signal of s_c for each flame particle is moved backward in time until the maximum correlation between $Ka(t)$ and $s_c(t + \Delta t)$ is reached (black dashed line on the bottom of Fig. 5). Thus, the time delay Δt is the time shift Δt_i for which $\max_{i=1,\dots,N} \left\{ \varrho\big(s_c(t)/s_{L,0}, Ka(t - \Delta t_i)\big) \right\}$, where $\varrho(a, b)$ is the Pearson correlation coefficient between the quantities a and b. An animation of this procedure is included in the supplementary materials. This time lag, however, is not constant, but is a function of the local time scales or unsteadiness of the flow.

To quantify the effect of local flow unsteadiness on the time delay between flame speed and flame stretch signal, a local time scale is defined for each flame particle. Because the flame particles selected here were chosen based on their lifetime which is dominated by a single frequency, the local time scale can be readily defined as the inverse frequency of the local flame stretch time signal f_K. More specifically, the frequency is approximated as twice the time between the first and last inflection points of the flame stretch signal (see the dotted red line in Fig. 5 at the bottom). With this, a local Damköhler number Da_K can be defined as

$$Da_K = \frac{1/f_K}{\tau_c}. \qquad (6)$$

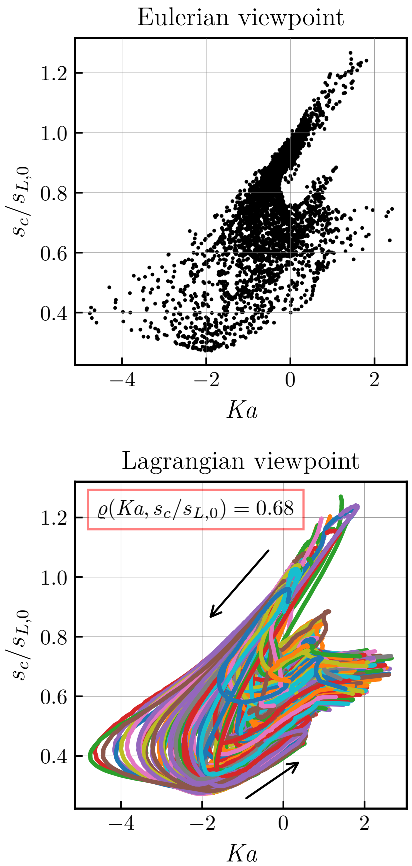

Fig. 4: Flame speed and flame stretch correlation in the Eulerian viewpoint (top) and Lagrangian viewpoint (bottom).

The dependence of the time lag between flame speed and flame stretch on the local time scale or Damköhler number is depicted in Fig. 6. Each point represents the time lag and local time scale extracted from a single flame particle from the chosen cluster tracking the flame surface during interaction with the turbulent flow. On the top, Δt is shown normalized by τ_c. The higher the local frequency, the lower the time delay Δt as the flame becomes less responsive to high frequency fluctuations with $Da_K < 1$. This is consistent with previous findings in oscillating laminar Bunsen and slot burner flames [1, 9]. The phase shift $\Delta\alpha = \Delta t / f_K^{-1}$ is shown at the bottom, which decreases approximately linearly in the log-log plot and approaches zero for $Da_K \to \infty$ or $f_K \to 0$. In the range of relevant Da_K for this flame, the phase shift is of the order $\Delta\alpha \approx \mathcal{O}(0.1 - 0.01)$.

To provide a more general definition of the local time scale than the one from the inflection point method, an alternative definition is introduced, which is based on the temporal rate of change of the flame stretch signal along the trajectory:

$$f_K \approx \frac{1}{4\tau_p \Delta Ka} \int \left| \frac{\partial Ka}{\partial\left(\frac{t}{\tau_c}\right)} \right| \mathrm{d}\left(\frac{t}{\tau_c}\right) \qquad (7)$$

where $\Delta Ka = (\max(Ka) - \min(Ka))$ and τ_p is the particle's lifetime. This expression yields the exact frequency in case the flame stretch time signal behaves like a harmonic oscillation for half a period. Plotting the normalized time shift for each particle with the local Damköhler number computed with Eq. 7 in Fig. 7 shows a weaker correlation compared to Fig. 6, but overall yields a qualitatively similar functional dependence.

Being able to model the time delay or memory effect for the local flame speed and flame stretch correlation presents a new approach of reducing the scattering of s_c and Ka significantly, which is usually present in turbulent flames. In contrast to Fig. 4 at the bottom, where instantaneous values of $s_c(t)$ and $Ka(t)$ from the FP trajectories are plotted without consideration of the memory effect resulting in a large scattering and low correlation coefficient $\varrho = 0.68$, Fig. 8 instead takes the time delay Δt into account. By correlating the instantaneous flame speed $s_c(t)$ with the flame stretch corrected by the time lag

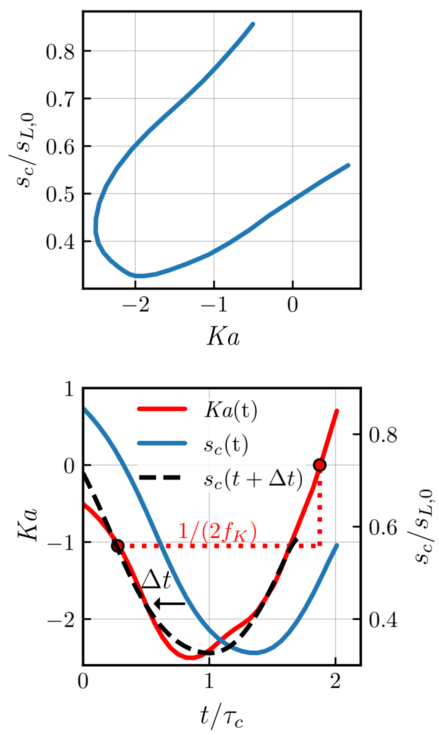

Fig. 5: Trajectory of a single flame particle in flame speed and flame stretch space (top) and recorded signals from the same flame particle of flame speed and flame stretch over time (bottom).

$Ka(t - \Delta t)$, a quasi-linear relation, analogous to a laminar flame, can be recovered with a high correlation coefficient of $\varrho = 0.92$. Moreover, the new quasi-linear correlation can be used to define a turbulent linear Markstein number [26–28]. Here, $Ma = -0.59$ averaged over the FP trajectories in the quasi-linear range. An additional comparison between the instantaneous and corrected flame particle trajectories in form of a joint probability density function is available in the supplementary materials.

It should be noted that recovering the quasi-linear correlation is only possible for a limited range of flame stretch. Figure 8 at the bottom shows that the linear correlation is not valid anymore for $|Ka| > 3$ in this case. This is expected, as the linear dependence of flame speed on flame stretch is generally only valid in the range of small Ka, which has been demonstrated for different laminar flame configurations, e.g. in [9, 29]. Therefore, the results obtained in this section are valid for local flame conditions that correspond to the flamelet regime and that fulfill the assumptions of the linear Markstein theory, i.e. covering a moderate range of flame stretch.

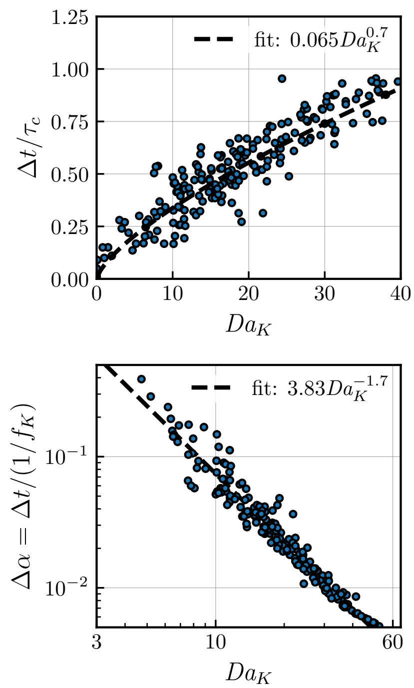

Fig. 6: Dependence of time lag Δt between local flame speed and flame stretch on the local Damköhler number. Time lag is plotted relative to τ_c at the top and the phase shift $\Delta\alpha$ at the bottom.

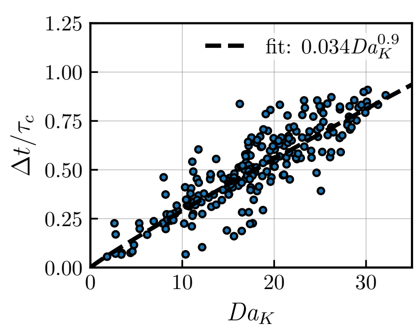

Fig. 7: Dependence of time lag Δt between local flame speed and flame stretch on the local Damköhler number using the definition from Eq. 7.

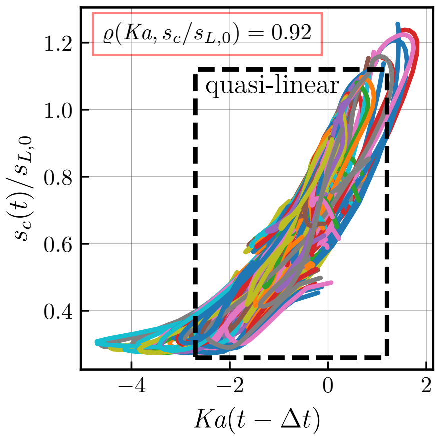

Fig. 8: Flame particle trajectories in flame speed and flame stretch space. Correlation of s_c and Ka after correcting the flame stretch signal with the time lag Δt.

6. Consumption Speed and Displacement Speed

In the analyses shown so far, flame speed has been expressed as the local flame consumption speed s_c. In general, recovering a quasi-linear correlation as shown in Fig. 8 is only possible for s_c but not for s_d. The reason lies in the way flame stretch affects the local equivalence ratios. The flame considered in this work is lean ($\phi < 1$) and the Lewis number below unity ($Le < 1$). Additionally, the flame is strongly affected by preferential diffusion, as shown e.g. by the existence of local extinction. Because of this, the main effect of flame stretch on this flame is a modification of the local equivalence ratio ϕ_{loc} by changing diffusive fluxes, or more specifically a decrease of ϕ_{loc} with increasing negative flame stretch. ϕ_{loc} is computed from the local elemental composition of the gas mixture at the FP position.

The following mechanism leads to the different behavior of s_c and s_d^*: (1) a flame interacting with a turbulent flow becomes stretched and curved; (2) the new flame stretch condition causes a change in diffusive species fluxes; (3) the altered diffusive fluxes cause a change in the local equivalence ratio. However, step (3) is not instantaneous. Instead, the flame requires some time to reach a quasi-steady state.

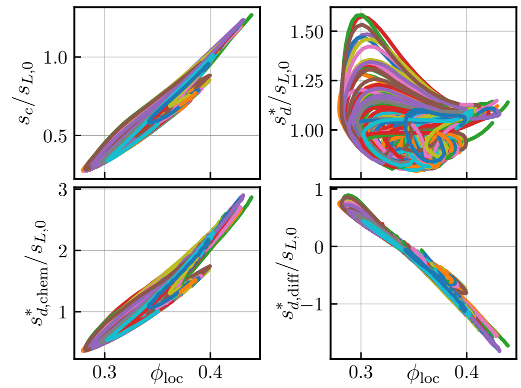

Fig. 9: Flame particle trajectories in the flame speed and local equivalence ratio space. Consumption speed (top left), total displacement speed (top right), contribution to s_d^* by chemical reactions (bottom left) and diffusion (bottom right).

Figure 9 illustrates this behavior. Depicted are the flame particle trajectories of instantaneous local consumption speed (top left), total displacement speed (top right) and the chemical and diffusive component of s_d^* (bottom) plotted against the instantaneous local equivalence ratio. Because s_c depends directly on the chemical reaction rates (see Eq. (4)), which in turn directly depend on ϕ_{loc}, there is a very strong correlation between s_c and ϕ_{loc}. Similarly, $s_{d,\mathrm{chem}}^*$ directly depends on $\dot{\omega}_F$ and thus ϕ_{loc}, and $s_{d,\mathrm{diff}}^*$ depends on the curvature and thus likewise affects ϕ_{loc}.

In this lean hydrogen flame, $s_{d,\mathrm{diff}}^*$ and $s_{d,\mathrm{chem}}^*$ have the opposite trend when correlated with ϕ_{loc}. Because of this, recovering a quasi-linear correlation between flame speed and flame stretch by taking the time delay Δt into account is possible for s_c, $s_{d,\mathrm{diff}}^*$ and $s_{d,\mathrm{chem}}^*$, but not s_d^* (see the respective figure in the supplementary materials). As a consequence, modeling s_d^* requires a separation into $s_{d,\mathrm{diff}}^*$ and $s_{d,\mathrm{chem}}^*$ when following the methodology from the previous section, in the case that $s_{d,\mathrm{diff}}^*$ and $s_{d,\mathrm{chem}}^*$ have a different trend with Ka or ϕ_{loc}.

7. Summary and Conclusions

A turbulent premixed hydrogen-air flame within the flamelet regime has been simulated. During the flame-turbulence interaction, flame particles (FPs) are tracked, which follow material points on the flame iso-surface. Due to the Lagrangian viewpoint enabled by the FPs, the effect of time histories on the local flame speed and flame stretch correlation can be examined. The key findings from this work are summarized as follows:

1. Although the hydrogen flame considered in this work is thermo-diffusively unstable, the characteristic life of flame particles found in methane and near-stoichiometric hydrogen flames has been confirmed to be present in this flame as well. Consumption speed s_c and displacement speed s_d behave oppositely in this flame, because s_c decreases with more negative flame stretch due to the reduction of local equivalence ratio and subsequent local extinction, while s_d increases due to high tangential diffusive fluxes caused by strong negative curvature.
2. Tracking points on the flame iso-surface over time reveals a time delay Δt between the flame speed and flame stretch time signal. Therefore, previous values of flame stretch affect currently observed values of flame speed.
3. The time delay Δt depends on the local time scale of the flow. By defining a local Damköhler number Da_K based on the frequency of the local flame stretch signal f_K, a strong correlation between Δt and Da_K is found. The higher the frequency, the shorter this time lag becomes as the flame has less time to relax to a quasi-steady state. The phase shift $\Delta t/f_K^{-1}$ on the other hand increases with increasing frequency or decreasing Damköhler number and approaches zero for $Da_K \to \infty$.
4. By taking the time delay into account, a quasi-linear correlation between flame speed and flame stretch can be recovered in turbulent flames from the otherwise strongly scattered data.
5. The recovery of a quasi-linear correlation is generally possible for the consumption speed and the two components of displacement speed, due to their strong correlation with the local equivalence ratio even in unsteady conditions, but not for the total displacement speed directly.

This work constitutes an important step toward new approaches of modeling local flame speed in turbulent flows based on local time scales and memory effects. By now, the methodology described in this work has been performed for points on the flame whose dynamics are temporarily dominated by a single frequency. While this allows for a simple definition of local time scales, the implications are relevant for the study of local flame dynamics in general. While the analysis of the memory effect in local flame dynamics has been performed in this work for a subset of FPs due to the complexity of the unsteady flame-flow interaction, further research is required to build new modeling concepts from these findings. Additional studies with more turbulent flames outside the flamelet regime will help to gain deeper insights into flame dynamics in the future.

Acknowledgments

This work utilized the computational resources ForHLR II and HoreKa at KIT funded by the Ministry of Science, Research and the Arts Baden-

Württemberg and DFG as well as the national supercomputer HPE Apollo Hawk at the High Performance Computing Center Stuttgart (HLRS). The work leading to this publication was supported by the PRIME programme of the German Academic Exchange Service (DAAD) with funds from the German Federal Ministry of Education and Research (BMBF).

References

[1] T. Zirwes, F. Zhang, Y. Wang, P. Habisreuther, J. Denev, Z. Chen, H. Bockhorn, D. Trimis, In-situ Flame Particle Tracking Based on Barycentric Coordinates for Studying Local Flame Dynamics in Pulsating Bunsen Flames, in: Proc. Combust. Inst., Vol. 38, Elsevier, 2021, pp. 2057–2066.

[2] T. Poinsot, D. Veynante, Theoretical and numerical combustion, RT Edwards, Inc., 2005.

[3] Z. Wang, J. Abraham, Effects of Karlovitz number on flame surface wrinkling in turbulent lean premixed methane-air flames, Comb. Sci. Tech. 190 (3) (2018) 363–392.

[4] Yuvraj, W. Song, H. Dave, H. G. Im, S. Chaudhuri, Local flame displacement speeds of hydrogen-air premixed flames in moderate to intense turbulence, Combust. Flame 236 (2022).

[5] J. H. Chen, H. G. Im, Correlation of flame speed with stretch in turbulent premixed methane/air flames, in: Symposium (International) on Combustion, Vol. 27, Elsevier, 1998, pp. 819–826.

[6] H. G. Im, J. H. Chen, Effects of flow transients on the burning velocity of laminar hydrogen/air premixed flames, Proc. Combust. Inst 28 (2) (2000) 1833–1840.

[7] N. Chakraborty, M. Klein, R. Cant, Stretch rate effects on displacement speed in turbulent premixed flame kernels in the thin reaction zones regime, Proc. Comb. Inst. 31 (1) (2007) 1385–1392.

[8] S. Hemchandra, T. Lieuwen, Local consumption speed of turbulent premixed flames–an analysis of "memory effects", Combust. Flame 157 (5) (2010) 955–965.

[9] F. Zhang, T. Zirwes, P. Habisreuther, H. Bockhorn, Effect of unsteady stretching on the flame local dynamics, Combust. Flame 175 (2017) 170–179.

[10] A. Herbert, U. Ahmed, N. Chakraborty, M. Klein, Applicability of extrapolation relations for curvature and stretch rate dependences of displacement speed for statistically planar turbulent premixed flames, Combustion Theory and Modelling 24 (6) (2020) 1021–1038.

[11] S. Chaudhuri, Life of flame particles embedded in premixed flames interacting with near isotropic turbulence, Proc. Combust. Inst. 35 (2) (2015) 1305–1312.

[12] H. A. Uranakara, S. Chaudhuri, H. L. Dave, P. G. Arias, H. G. Im, A flame particle tracking analysis of turbulence–chemistry interaction in hydrogen–air premixed flames, Combust. Flame 163 (2016) 220–240.

[13] S. Chaudhuri, Global and local viewpoints to analyze turbulence-premixed flame interaction, in: Combustion for Power Generation and Transportation, Springer, 2017, pp. 101–123.

[14] H. L. Dave, A. Mohan, S. Chaudhuri, Genesis and evolution of premixed flames in turbulence, Combust. Flame 196 (2018) 386–399.

[15] S. Pope, The evolution of surfaces in turbulence, Int. J. of engineering science 26 (5) (1988) 445–469.

[16] F. C. C. Galeazzo, F. Zhang, T. Zirwes, P. Habisreuther, H. Bockhorn, N. Zarzalis, D. Trimis, Implementation of an efficient synthetic inflow turbulence-generator in the open-source code openfoam for 3d les/dns applications, in: High Performance Computing in Science and Engineering'20, Springer, 2021, pp. 207–221.

[17] F. Zhang, H. Bonart, T. Zirwes, P. Habisreuther, H. Bockhorn, N. Zarzalis, Direct numerical simulation of chemically reacting flows with the public domain code OpenFOAM, in: W. Nagel, D. Kröner, M. Resch (Eds.), High Performance Computing in Science and Engineering '14, Springer Berlin Heidelberg, 2015, pp. 221–236.

[18] T. Zirwes, F. Zhang, P. Habisreuther, M. Hansinger, H. Bockhorn, M. Pfitzner, D. Trimis, Quasi-dns dataset of a piloted flame with inhomogeneous inlet conditions, Flow, Turb. and Combust. (2019).

[19] T. Zirwes, T. Häber, F. Zhang, H. Kosaka, A. Dreizler, M. Steinhausen, C. Hasse, A. Stagni, D. Trimis, R. Suntz, et al., Numerical study of quenching distances for side-wall quenching using detailed diffusion and chemistry, Flow, Turbulence and Combustion 106 (2) (2021) 649–679.

[20] T. Zirwes, F. Zhang, J. Denev, P. Habisreuther, H. Bockhorn, Automated Code Generation for Maximizing Performance of Detailed Chemistry Calculations in OpenFOAM, in: W. Nagel, D. Kröner, M. Resch (Eds.), High Performance Computing in Science and Engineering '17, Springer, 2017, pp. 189–204.

[21] T. Zirwes, F. Zhang, J. Denev, P. Habisreuther, H. Bockhorn, D. Trimis, Improved Vectorization for Efficient Chemistry Computations in OpenFOAM for Large Scale Combustion Simulations, in: W. Nagel, D. Kröner, M. Resch (Eds.), High Performance Computing in Science and Engineering '18, Springer, 2018, pp. 209–224.

[22] H. Weller, G. Tabor, H. Jasak, C. Fureby, OpenFOAM, openCFD ltd., https://openfoam.org (2017).

[23] D. Goodwin, H. Moffat, R. Speth, Cantera: An object-oriented software toolkit for chemical kinetics, thermodynamics, and transport processes, http://www.cantera.org (2017).

[24] J. Li, Z. Zhao, A. Kazakov, F. L. Dryer, An updated comprehensive kinetic model of hydrogen combustion, Int. J. of Chem. Kin. 36 (10) (2004) 566–575.

[25] H. L. Dave, S. Chaudhuri, Evolution of local flame displacement speeds in turbulence, Journal of Fluid Mechanics 884 (2020).

[26] D. Bradley, Problems of predicting turbulent burning rates, Combustion Theory and Modelling 6 (2) (2002) 361.

[27] J. F. Driscoll, Turbulent premixed combustion: Flamelet structure and its effect on turbulent burning velocities, Progress in Energy and Combustion Science 34 (1) (2008) 91–134.

[28] M. Weiß, N. Zarzalis, R. Suntz, Experimental study of Markstein number effects on laminar flamelet velocity in turbulent premixed flames, Combustion and Flame 154 (4) (2008) 671–691.

[29] A. P. Kelley, C. K. Law, Nonlinear effects in the extraction of laminar flame speeds from expanding spherical flames, Combustion and Flame 156 (9) (2009) 1844–1851.